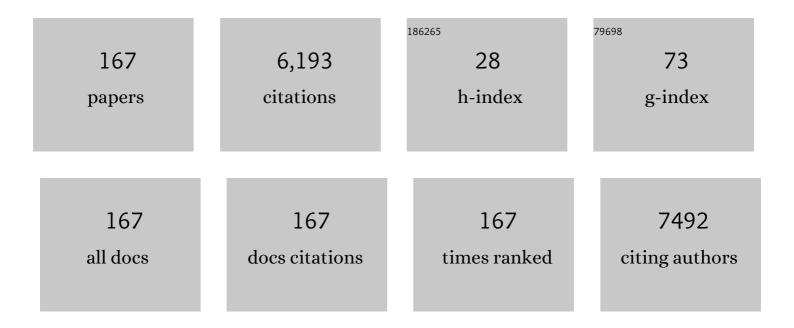
List of Publications by Year in descending order

Source: https://exaly.com/author-pdf/8102281/publications.pdf Version: 2024-02-01



#	Article	IF	CITATIONS
1	Solar cell efficiency tables (version 54). Progress in Photovoltaics: Research and Applications, 2019, 27, 565-575.	8.1	1,096
2	Solar cell efficiency tables (Version 55). Progress in Photovoltaics: Research and Applications, 2020, 28, 3-15.	8.1	694
3	Solar cell efficiency tables (Version 53). Progress in Photovoltaics: Research and Applications, 2019, 27, 3-12.	8.1	655
4	Solar cell efficiency tables (version 56). Progress in Photovoltaics: Research and Applications, 2020, 28, 629-638.	8.1	461
5	Solar cell efficiency tables (Version 60). Progress in Photovoltaics: Research and Applications, 2022, 30, 687-701.	8.1	406
6	Solar cell efficiency tables (Version 58). Progress in Photovoltaics: Research and Applications, 2021, 29, 657-667.	8.1	363
7	Solar cell efficiency tables (version 59). Progress in Photovoltaics: Research and Applications, 2022, 30, 3-12.	8.1	253
8	Intersubband absorption linewidth in GaAs quantum wells due to scattering by interface roughness, phonons, alloy disorder, and impurities. Journal of Applied Physics, 2003, 93, 1586-1597.	2.5	217
9	Effects of interface roughness and phonon scattering on intersubband absorption linewidth in a GaAs quantum well. Applied Physics Letters, 2001, 78, 3448-3450.	3.3	84
10	High collection efficiency in fluorescence microscopy with a solid immersion lens. Applied Physics Letters, 1999, 75, 1667-1669.	3.3	75
11	Thorough subcells diagnosis in a multi-junction solar cell via absolute electroluminescence-efficiency measurements. Scientific Reports, 2015, 5, 7836.	3.3	74
12	Lasing from a single-quantum wire. Applied Physics Letters, 2002, 81, 4937-4939.	3.3	58
13	Aberrations and allowances for errors in a hemisphere solid immersion lens for submicron-resolution photoluminescence microscopy. Journal of Applied Physics, 1999, 85, 6923-6925.	2.5	52
14	Voltage-Dependent Temperature Coefficient of the I–V Curves of Crystalline Silicon Photovoltaic Modules. IEEE Journal of Photovoltaics, 2018, 8, 48-53.	2.5	51
15	Application of solid immersion lens to high-spatial resolution photoluminescence imaging of GaAs quantum wells at low temperatures. Applied Physics Letters, 1998, 73, 635-637.	3.3	47
16	Quantum wells with atomically smooth interfaces. Applied Physics Letters, 2002, 81, 49-51.	3.3	47
17	Influence of N, O and C impurities in a-Si:H. Journal of Non-Crystalline Solids, 1991, 137-138, 391-394.	3.1	42
18	Photoluminescence of CdS:Mn2+ and Eu3+ nanoparticles dispersed in zirconia sol–gel films. Journal of Luminescence, 2000, 87-89, 478-481.	3.1	42

#	Article	IF	CITATIONS
19	Doping effect of oxygen or nitrogen impurity in hydrogenated amorphous silicon films. Applied Physics Letters, 1991, 59, 2130-2132.	3.3	41
20	Biexciton Gain and the Mott Transition in GaAs Quantum Wires. Physical Review Letters, 2007, 99, 167403.	7.8	41
21	One-dimensional continuum and exciton states in quantum wires. Applied Physics Letters, 2003, 82, 379-381.	3.3	34
22	Conversion efficiency limits and bandgap designs for multi-junction solar cells with internal radiative efficiencies below unity. Optics Express, 2016, 24, A740.	3.4	34
23	Stimulated emission in ridge quantum wire laser structures measured with optical pumping and microscopic imaging methods. Applied Physics Letters, 1998, 73, 511-513.	3.3	33
24	Observation of large many-body Coulomb interaction effects in a doped quantum wire. Solid State Communications, 2002, 122, 169-173.	1.9	33
25	Degradation mechanism of perovskite CH ₃ NH ₃ Pbl ₃ diode devices studied by electroluminescence and photoluminescence imaging spectroscopy. Applied Physics Express, 2015, 8, 102302.	2.4	31
26	Coulomb-correlated electron-hole plasma and gain in a quantum-wire laser of high uniformity. Physical Review B, 2003, 67, .	3.2	29
27	Subcycle Optical Response Caused by a Terahertz Dressed State with Phase-Locked Wave Functions. Physical Review Letters, 2016, 117, 277402.	7.8	29
28	Scanning tunneling spectroscopy of n-type GaAs under laser irradiation. Applied Physics Letters, 1997, 70, 2162-2164.	3.3	28
29	Large terrace formation and modulated electronic states in (110) GaAs quantum wells. Physical Review B, 2001, 63, .	3.2	28
30	Impact of sub-cell internal luminescence yields on energy conversion efficiencies of tandem solar cells: A design principle. Applied Physics Letters, 2014, 104, 031118.	3.3	28
31	Formation of Flat Monolayer-Step-Free (110) GaAs Surfaces by Growth Interruption Annealing during Cleaved-Edge Epitaxial Overgrowth. Japanese Journal of Applied Physics, 2001, 40, L252-L254.	1.5	27
32	Polarization-dependent photoluminescence-excitation spectra of one-dimensional exciton and continuum states in T-shaped quantum wires. Applied Physics Letters, 2003, 83, 2043-2045.	3.3	27
33	Fourier imaging study of efficient near-field optical coupling in solid immersion fluorescence microscopy. Journal of Applied Physics, 2002, 92, 862-865.	2.5	26
34	Low and anisotropic barrier energy for adatom migration on a GaAs (110) surface studied by first-principles calculations. Applied Physics Letters, 2003, 83, 4187-4189.	3.3	26
35	Sub-5-ps optical pulse generation from a 155-µm distributed-feedback laser diode with nanosecond electric pulse excitation and spectral filtering. Optics Express, 2012, 20, 24843.	3.4	25
36	Spectral dynamics of picosecond gain-switched pulses from nitride-based vertical-cavity surface-emitting lasers. Scientific Reports, 2014, 4, 4325.	3.3	25

#	Article	IF	CITATIONS
37	Characterizations of Radiation Damage in Multijunction Solar Cells Focused on Subcell Internal Luminescence Quantum Yields via Absolute Electroluminescence Measurements. IEEE Journal of Photovoltaics, 2016, 6, 777-782.	2.5	25
38	Translation of Solar Cell Performance for Irradiance and Temperature From a Single <i>I-V</i> Curve Without Advance Information of Translation Parameters. IEEE Journal of Photovoltaics, 2019, 9, 1195-1201.	2.5	25
39	Microphotoluminescence characterization of cleaved edge overgrowth T-shaped InxGa1â^'xAs quantum wires. Journal of Applied Physics, 1998, 83, 3777-3783.	2.5	24
40	Atomically Engineered Metal–Insulator Transition at the TiO ₂ /LaAlO ₃ Heterointerface. Nano Letters, 2014, 14, 6743-6746.	9.1	24
41	Solar-cell radiance standard for absolute electroluminescence measurements and open-circuit voltage mapping of silicon solar modules. Journal of Applied Physics, 2016, 119, .	2.5	24
42	Solid-immersion photoluminescence microscopy of carrier diffusion and drift in facet-growth GaAs quantum wells. Applied Physics Letters, 1998, 73, 2965-2967.	3.3	23
43	Tunneling spectroscopic study of InAs-covered GaAs under laser irradiation. Applied Physics A: Materials Science and Processing, 1998, 66, S1055-S1058.	2.3	22
44	Application of Solid Immersion Lens to High-Resolution Photoluminescence Imaging of Patterned GaAs Quantum Wells. Japanese Journal of Applied Physics, 1997, 36, L962-L964.	1.5	21
45	Photoluminescence study of lateral confinement energy in T-shapedInxGa1â^'xAsquantum wires. Physical Review B, 1998, 57, 3765-3768.	3.2	19
46	Strong photoabsorption by a single-quantum wire in waveguide-transmission spectroscopy. Applied Physics Letters, 2005, 86, 243101.	3.3	19
47	Gain-switched pulses from InGaAs ridge-quantum-well lasers limited by intrinsic dynamical gain suppression. Optics Express, 2013, 21, 7570.	3.4	19
48	Temperature dependence of the short circuit current and spectral responsivity of various kinds of crystalline silicon photovoltaic devices. Japanese Journal of Applied Physics, 2018, 57, 08RG17.	1.5	19
49	Temperature and irradiance dependences of the current and voltage at maximum power of crystalline silicon PV devices. Solar Energy, 2020, 204, 459-465.	6.1	19
50	Exciton-plasma crossover with electron-hole density in T-shaped quantum wires studied by the photoluminescence spectrograph method. Physical Review B, 2006, 74, .	3.2	18
51	Metal-to-insulator transition in anatase TiO2 thin films induced by growth rate modulation. Applied Physics Letters, 2012, 101, .	3.3	18
52	Step-edge kinetics driving the formation of atomically flat (110) GaAs surfaces. Applied Physics Letters, 2003, 82, 1709-1711.	3.3	17
53	Improved High Collection Efficiency in Fluorescence Microscopy with a Weierstrass-Sphere Solid Immersion Lens. Japanese Journal of Applied Physics, 2002, 41, L858-L860.	1.5	16
54	Twin photoluminescence peaks from single isoelectronic traps in nitrogen δ-doped GaAs. Physica E: Low-Dimensional Systems and Nanostructures, 2008, 40, 2110-2112.	2.7	16

#	Article	IF	CITATIONS
55	Thermal-equilibrium relation between the optical emission and absorption spectra of a doped semiconductor quantum well. Physical Review B, 2009, 80, .	3.2	16
56	Dynamics of short-pulse generation via spectral filtering from intensely excited gain-switched 155-μm distributed-feedback laser diodes. Optics Express, 2013, 21, 10597.	3.4	16
57	Femtosecond pulse generation beyond photon lifetime limit in gain-switched semiconductor lasers. Communications Physics, 2018, 1, .	5.3	16
58	Time-resolved observation of coherent excitonic nonlinear response with a table-top narrowband THz pulse wave. Applied Physics Letters, 2015, 107, 221106.	3.3	15
59	One-Dimensional Band-Edge Absorption in a Doped Quantum Wire. Physical Review Letters, 2007, 99, 126803.	7.8	14
60	Photoluminescence from single isoelectronic traps in nitrogen delta-doped GaAs grown on GaAs(111)A. Physica E: Low-Dimensional Systems and Nanostructures, 2010, 42, 2529-2531.	2.7	14
61	Observation of high Rydberg states of one-dimensional excitons in GaAs quantum wires by magnetophotoluminescence excitation spectroscopy. Physical Review B, 2012, 86, .	3.2	14
62	Transient hot-carrier optical gain in a gain-switched semiconductor laser. Applied Physics Letters, 2013, 103, .	3.3	14
63	Detection of shading effect by using the current and voltage at maximum power point of crystalline silicon PV modules. Solar Energy, 2020, 211, 1365-1372.	6.1	14
64	Laser irradiation effects on tunneling properties of nâ€ŧype GaAs and InAs by scanning tunneling microscopy. Applied Physics Letters, 1996, 68, 3479-3481.	3.3	13
65	Selective molecular beam epitaxy (MBE) growth of GaAs/AlAs ridge structures containing 10nm scale wires and side quantum wells (QWs) and their stimulated emission characteristics. Journal of Crystal Growth, 1999, 201-202, 810-813.	1.5	13
66	Room-temperature excitonic absorption in quantum wires. Applied Physics Letters, 2005, 87, 223119.	3.3	12
67	Blue 6-ps short-pulse generation in gain-switched InGaN vertical-cavity surface-emitting lasers via impulsive optical pumping. Applied Physics Letters, 2012, 101, .	3.3	12
68	High-precision group-delay dispersion measurements of optical fibers via fingerprint-spectral wavelength-to-time mapping. Photonics Research, 2016, 4, 13.	7.0	12
69	Improvements in world-wide intercomparison of PV module calibration. Solar Energy, 2017, 155, 1451-1461.	6.1	12
70	Micro-photoluminescence study of nitrogen delta-doped GaAs grown by metalorganic vapor phase epitaxy. Journal of Crystal Growth, 2007, 298, 73-75.	1.5	11
71	Comparative Study of Power Generation in Curved Photovoltaic Modules of Series- and Parallel-Connected Solar Cells. IEEE Journal of Photovoltaics, 2021, 11, 708-714.	2.5	11
72	Scanning tunneling microscopy of undoped GaAs/AlGaAs heterostructures under laser irradiation. Applied Physics Letters, 1996, 68, 502-504.	3.3	10

#	Article	IF	CITATIONS
73	Imaging of emission patterns in a T-shaped quantum wire laser. Applied Physics Letters, 2003, 83, 4089-4091.	3.3	10
74	Mode locking of a GaInN semiconductor laser with an internal saturable absorber. Applied Physics Letters, 2009, 94, .	3.3	10
75	Absolute electroluminescence imaging of multi-junction solar cells and calibration standards. , 2015, , .		10
76	Direct generation of 2-ps blue pulses from gain-switched InGaN VCSEL assessed by up-conversion technique. Scientific Reports, 2015, 4, 6401.	3.3	10
77	Absolute bioluminescence imaging at the single-cell level with a light signal at the Attowatt level. BioTechniques, 2018, 64, 270-274.	1.8	10
78	Control of MBE surface step-edge kinetics to make an atomically smooth quantum well. Journal of Crystal Growth, 2003, 251, 62-67.	1.5	9
79	Surface-morphology evolution during growth-interrupt in situ annealing on GaAs(110) epitaxial layers. Journal of Applied Physics, 2007, 101, 103541.	2.5	9
80	Temperature-dependent current injection and lasing in T-shaped quantum-wire laser diodes with perpendicular p- and n-doping layers. Applied Physics Letters, 2007, 90, 091108.	3.3	9
81	Gain-switching dynamics in optically pumped single-mode InGaN vertical-cavity surface-emitting lasers. Optics Express, 2014, 22, 4196.	3.4	9
82	Diagnosis of GaInAs/GaAsP Multiple Quantum Well Solar Cells With Bragg Reflectors via Absolute Electroluminescence. IEEE Journal of Photovoltaics, 2017, 7, 781-786.	2.5	9
83	Analysis of Gain-Switching Characteristics Including Strong Gain Saturation Effects in Low-Dimensional Semiconductor Lasers. Japanese Journal of Applied Physics, 2012, 51, 098001.	1.5	9
84	Microscopy of electronic states contributing to lasing in ridge quantum-wire laser structure. Applied Physics Letters, 1999, 75, 2190-2192.	3.3	8
85	Photoluminescence properties and ultra-fast decay profiles of nanoparticles in sol–gel zirconia thin films xZrO2·100â^'x Cds:Mn2+ and Eu3+. Journal of Luminescence, 2001, 94-95, 191-195.	3.1	8
86	Analysis of Gain-Switching Characteristics Including Strong Gain Saturation Effects in Low-Dimensional Semiconductor Lasers. Japanese Journal of Applied Physics, 2012, 51, 098001.	1.5	8
87	Biexciton Luminescence from Individual Isoelectronic Traps in Nitrogen \$delta\$-Doped GaAs. Applied Physics Express, 2012, 5, 111201.	2.4	8
88	Picosecond tunable gain-switched blue pulses from GaN laser diodes with nanosecond current injections. Optics Express, 2017, 25, 13046.	3.4	8
89	Photoreflectance spectra from a surface and an interface of n-type GaAs epitaxial layers and their modulation frequency dependence. Applied Surface Science, 1997, 115, 347-354.	6.1	7
90	Polarization Dependence of the Optical Interband Transition Defined by the Spatial Variation of the Valencep-Orbital Bloch Functions in Quantum Wires. Japanese Journal of Applied Physics, 2002, 41, 5924-5936.	1.5	7

#	Article	IF	CITATIONS
91	Light-emitting-diode Lambertian light sources as low-radiant-flux standards applicable to quantitative luminescence-intensity imaging. Review of Scientific Instruments, 2017, 88, 093704.	1.3	7
92	One-dimensional excitonic states and lasing in highly uniform quantum wires formed by cleaved-edge overgrowth with growth-interrupt annealing. Journal of Physics Condensed Matter, 2004, 16, S3549-S3566.	1.8	6
93	Robust Carrier-Induced Suppression of Peak Gain Inherent to Quantum-Wire Lasers. Journal of the Physical Society of Japan, 2011, 80, 114716.	1.6	6
94	Fano-Resonance Gain by Dephasing Electron–Hole Cooper Pairs in Semiconductors. Journal of the Physical Society of Japan, 2012, 81, 093706.	1.6	6
95	Quantitative absorption spectra of quantum wires measured by analysis of attenuated internal emissions. Applied Physics Letters, 2012, 100, 112101.	3.3	6
96	Intrinsic radiative lifetime derived via absorption cross section of one-dimensional excitons. Scientific Reports, 2013, 3, 1941.	3.3	6
97	Improved precision of the outdoor performance measurements of photovoltaic modules by using the photovoltaic irradiance sensor. Solar Energy, 2020, 211, 82-89.	6.1	6
98	Effect of Charged Defects on Properties of Amorphous Si-Based Alloys. Japanese Journal of Applied Physics, 1990, 29, L1578-L1581.	1.5	5
99	Application of Solid Immersion Lens to Submicron Resolution Imaging of Nano-Scale Quantum Wells. Optical Review, 1999, 6, 257-260.	2.0	5
100	Intersubband electronic Raman scattering in narrow GaAs single quantum wells dominated by single-particle excitations. Physical Review B, 2004, 70, .	3.2	5
101	Photoluminescence study of isoelectronic traps in dilute GaAsN alloys. Physica Status Solidi C: Current Topics in Solid State Physics, 2007, 4, 2760-2763.	0.8	5
102	Broadband tunable integrated CMOS pulser with 80-ps minimum pulse width for gain-switched semiconductor lasers. Scientific Reports, 2017, 7, 6878.	3.3	5
103	Characterization of Cleaved GaAs Tips for Scanning Tunneling Microscopy. Japanese Journal of Applied Physics, 1997, 36, 6957-6961.	1.5	4
104	Quantum wire lasers with high uniformity formed by cleaved-edge overgrowth with growth-interrupt anneal. Solid State Communications, 2003, 127, 63-68.	1.9	4
105	Fabrication of Thin Films Using a Soluble Metal Phthalocyanine Salt and Their Photoconductive Properties. Chemistry Letters, 2003, 32, 130-131.	1.3	4
106	Formation mechanisms of monolayer pits having characteristic step-edge shapes on annealed GaAs (110) surfaces. Thin Solid Films, 2004, 464-465, 38-41.	1.8	4
107	Fabrication and microscopic characterization of a single quantum-wire laser with high uniformity. Physica E: Low-Dimensional Systems and Nanostructures, 2004, 21, 230-235.	2.7	4
108	Micro-photoluminescence characterizations of GaInAsP/InP single quantum wires fabricated by dry etching and regrowth. Journal of Applied Physics, 2007, 102, .	2.5	4

#	Article	IF	CITATIONS
109	Transient gain analysis of gain-switched semiconductor lasers during pulse lasing. Applied Optics, 2015, 54, 10438.	2.1	4
110	Transient Analysis of Ion-Migration Current for Degradation Diagnostics of Perovskite Solar Cells. IEEE Journal of Photovoltaics, 2022, 12, 1170-1174.	2.5	4
111	Fabrication and optical properties of GaAs/AlGaAs quantum dot grown in tetrahedral-shaped recesses on GaAs B substrates by MOVPE. Physica E: Low-Dimensional Systems and Nanostructures, 2000, 7, 308-316.	2.7	3
112	Collective and single-particle intersubband excitations in narrow quantum wells selected by infrared absorption and resonant Raman scattering. Physical Review B, 2006, 74, .	3.2	3
113	Carrierâ€densityâ€dependent increase and suppression of optical gain in Tâ€shaped quantumâ€wire lasers. Physica Status Solidi C: Current Topics in Solid State Physics, 2008, 5, 2841-2843.	0.8	3
114	Exciton–biexciton-plasma crossover and formation of optical gain in quantum wires. Physica E: Low-Dimensional Systems and Nanostructures, 2008, 40, 1726-1728.	2.7	3
115	Coulombâ€modulated gain spectra in currentâ€njection Tâ€shaped quantumâ€wire lasers. Physica Status Solidi C: Current Topics in Solid State Physics, 2011, 8, 20-23.	0.8	3
116	Applicability of continuum absorption in semiconductor quantum wells to absolute absorption-strength standards. Applied Physics Letters, 2012, 101, 032108.	3.3	3
117	Calibration standards and measurement accuracy of absolute electroluminescence and internal properties in multi-junction and arrayed solar cells. Proceedings of SPIE, 2016, , .	0.8	3
118	Characterization and modeling of radiation damages via internal radiative efficiency in multi-junction solar cells. Proceedings of SPIE, 2016, , .	0.8	3
119	Coherent detection of THz-induced sideband emission from excitons in the nonperturbative regime. Physical Review B, 2018, 97, .	3.2	3
120	Simulation of Diffuse Irradiance Impact on Energy Yield of Curved Photovoltaic Modules Using Climatic Datasets. IEEE Journal of Photovoltaics, 2022, 12, 526-532.	2.5	3
121	Carrier diffusion on atomically flat () GaAs quantum wells. Physica E: Low-Dimensional Systems and Nanostructures, 2004, 21, 689-692.	2.7	2
122	Photo-induced improvement of radiative efficiency and structural changes in GaAsN alloys. Physica Status Solidi C: Current Topics in Solid State Physics, 2006, 3, 1907-1910.	0.8	2
123	Low-Threshold Current-Injection Single-Mode Lasing in T-shaped GaAs/AlGaAs Quantum Wires. Japanese Journal of Applied Physics, 2007, 46, L330-L332.	1.5	2
124	Micro-Raman study on the improvement of luminescence efficiency of GaAsN alloys. Journal of Crystal Growth, 2007, 298, 131-134.	1.5	2
125	Current-injection T-shaped quantum wire lasers with perpendicular doping layers operating at 100K. Physica E: Low-Dimensional Systems and Nanostructures, 2008, 40, 1947-1949.	2.7	2
126	Measurements of Cavity-Length-Dependent Internal Differential Quantum Efficiency and Internal Optical Loss in Laser Diodes. Japanese Journal of Applied Physics, 2008, 47, 2288.	1.5	2

#	Article	IF	CITATIONS
127	Measurements of Gain Spectra over Wide Spectral Ranges in GalnAsP/InP Multiple-Quantum-Well Laser Diodes. Japanese Journal of Applied Physics, 2008, 47, 329-333.	1.5	2
128	Single Photon Generation from Nitrogen Atomic-Layer Doped Gallium Arsenide. Materials Science Forum, 0, 706-709, 2916-2921.	0.3	2
129	Double-Core-Slab-Waveguide Semiconductor Lasers for End Optical Pumping. Applied Physics Express, 2013, 6, 062702.	2.4	2
130	Conversion efficiency limits and optimized designs for tandem solar cells with realistic sub-cell material quality. , 2014, , .		2
131	Multi-junction-solar-cell designs and characterizations based on detailed-balance principle and luminescence yields. Proceedings of SPIE, 2015, , .	0.8	2
132	Current leakage and fill factor in multi-junction solar cells linked via absolute electroluminescence characterization. , 2016, , .		2
133	Accuracy evaluations for standardization of multi-junction solar-cell characterizations via absolute electroluminescence. , 2017, , .		2
134	Corrections to "Translation of Solar Cell Performance for Irradiance and Temperature From a Single I-V Curve Without Advance Information of Translation Parameters―[Sep 19 1195-1201]. IEEE Journal of Photovoltaics, 2020, 10, 912-912.	2.5	2
135	Vertically polarized lasing and photoluminescence in a ridge quantum-wire laser. Physical Review B, 2003, 68, .	3.2	1
136	Micro-photoluminescence characterization of local electronic states in a (110) GaAs quantum well fabricated by cleaved-edge overgrowth. Journal of Applied Physics, 2004, 96, 6370-6374.	2.5	1
137	Electronic structure and efficient carrier injection in low-threshold T-shaped quantum-wire lasers with parallel p- and n-doping layers. Journal of Applied Physics, 2007, 102, 043108.	2.5	1
138	Waveguide Two-Point Differential-Excitation Method for Quantitative Absorption Measurements of Nanostructures. Japanese Journal of Applied Physics, 2012, 51, 106601.	1.5	1
139	Fluorescent Radiation Thermometry at Cryogenic Temperatures Based on Detailed Balance Relation. Applied Physics Express, 2013, 6, 056602.	2.4	1
140	Waveguide Two-Point Differential-Excitation Method for Quantitative Absorption Measurements of Nanostructures. Japanese Journal of Applied Physics, 2012, 51, 106601.	1.5	1
141	Precise performance diagnosis of photovoltaic string by operation voltage and current: Experimental verification. Solar Energy, 2021, 230, 704-713.	6.1	1
142	Round-Robin Inter-Comparison of Maximum Power Measurement for Metastable Perovskite Solar Cells. ECS Journal of Solid State Science and Technology, 2022, 11, 055008.	1.8	1
143	Fluorination and superconductivity of T' phase Nd2CuO4â^'y. Physica C: Superconductivity and Its Applications, 1991, 185-189, 613-614.	1.2	0
144	Publisher's Note:â€,Vertically polarized lasing and photoluminescence in a ridge quantum-wire laser [Phys. Rev. B68, 193304 (2003)]. Physical Review B, 2004, 69, .	3.2	0

#	Article	IF	CITATIONS
145	Improvement of Interface Quality in Cleaved-Edge-Overgrowth GaAs Quantum Wires Based on Micro-optical Characterization. , 2005, , 43-82.		Ο
146	Crossover from Excitons to an Electron-Hole Plasma in a High-Quality Single T-Shaped Quantum Wire. AIP Conference Proceedings, 2005, , .	0.4	0
147	Optical gain spectra due to a one-dimensional electron-hole plasma in quantum-wire lasers. AIP Conference Proceedings, 2005, , .	0.4	0
148	Photoluminescence of GaInAsP/InP Single Quantum Wires With Lateral Widths Down To 6 nm Fabricated by Dry Etching and Regrowth. , 2007, , .		0
149	Gain Characteristics of Coulomb-Correlated Quantum Wire. , 2007, , .		Ο
150	Density tuning of one-dimensional electron gas in a T-shaped quantum wire. , 2007, , .		0
151	Surface stability and atomic-step-edge kinetics on a cleaved-edge-overgrown (110) GaAs surface. AIP Conference Proceedings, 2007, , .	0.4	Ο
152	Low-Threshold Current-Injection Single-Mode Lasing in T-shaped Quantum Wires with Parallel Doping Layer. , 2007, , .		0
153	Linear optical responses of one-dimensional electron systems: Comparison of theories with experiments. Physica E: Low-Dimensional Systems and Nanostructures, 2008, 40, 1288-1291.	2.7	Ο
154	Micro-photoluminescence excitation spectroscopy on asymmetric absorption line shapes of weakly localized excitons in a quantum well. Solid State Communications, 2008, 147, 114-117.	1.9	0
155	Optical Detection of Electron-Depletion Region Surrounding Metal Electrode on a Dilute Two-Dimensional Electron Gas. Japanese Journal of Applied Physics, 2008, 47, 4496-4498.	1.5	Ο
156	Optical Waveguide-Transmission Spectroscopy of One-Dimensional Excitons in T-shaped Quantum Wires. , 2011, , .		0
157	Biexciton emission from single isoelectronic traps formed by nitrogen-nitrogen pairs in GaAs. , 2013, , .		Ο
158	Mode imaging and loss evaluation of semiconductor waveguides. Review of Scientific Instruments, 2014, 85, 053109.	1.3	0
159	Balance sheets of energy and carriers and subcell characteristics in a GaInP/GaAs/Ge tandem solar cell. , 2014, , .		Ο
160	Gain switching of a double-core-waveguide semiconductor laser via traveling-wave optical pumping. Applied Physics Express, 2014, 7, 062701.	2.4	0
161	Characterizations of radiation damages in multi-junction solar cells focused on subcell internal luminescence quantum yields via absolute electroluminescence measurements. , 2015, , .		0
162	Time-resolved observation of excitonic dynamics under coherent terahertz excitation in GaAs quantum wells. , 2015, , .		0

#	Article	IF	CITATIONS
163	Notice of Removal Diagnosis of GalnAs multiple-quantum-well solar cells with Bragg reflectors via absolute electroluminescence. , 2017, , .		0
164	Effect of solar cell interconnections on curved photovoltaic module performance. , 2021, , .		0
165	Report on CLEO/QELS 2000. The Review of Laser Engineering, 2000, 28, 526-547.	0.0	0
166	Single-particle Nature of Intersubband Electronic Raman Scattering and Dynamical Many-body Effects in Narrow GaAs Quantum Wells. AIP Conference Proceedings, 2007, , .	0.4	0
167	Current-injection lasing in T-shaped GaAs/AlGaAs quantum-wire lasers. AIP Conference Proceedings, 2007, , .	0.4	0